



Western Montana Snow Squall Climatology and Synoptic Patterns, 2000–2020

ALEX E. LUKINBEAL
NOAA/National Weather Service, Missoula, MT

(Manuscript received 13 October 2022; review completed 6 November 2023)

ABSTRACT

The rapid onset of whiteout conditions, from strong winds, blowing snow, and heavy snow, associated with snow squalls often results in hazardous travel conditions. Snow squalls bring pronounced impacts to the transportation sector, leading to accidents, fatalities, and significant travel delays. Given these impacts, historical frequencies, and the synoptic environments associated with snow squalls in western Montana were examined to develop forecast aides, primarily through synoptic pattern recognition, for meteorologists to identify and communicate snow squalls. A 20-yr climatology was constructed to identify events characterized by wind gusts ≥ 26 kt (30 mph) and visibility ≤ 0.8 km (0.5 mi). 74 snow squall events were identified from 2000 through 2020 across three ASOS sites: Missoula (KMSO), Kalispell (KGPI), and Butte (KBTM). The median duration of heavy (moderate) snow during snow squalls was 26 (34) min. A composite study utilizing these events was conducted using the NCEP North American Regional Reanalysis. The composite study along with surface observations, revealed three distinct snow squall patterns and types: orographic snow bands, Pacific cold fronts, and Canadian arctic fronts.

1. Introduction

The abrupt onset of heavy snow, gusty winds, and falling temperatures associated with snow squalls often leads to dangerous travel conditions. Transportation impacts are profound and stem from the combination of low visibility and slippery road conditions often associated with a flash freeze of the road surface during snow squall events. Multi-vehicle accidents and pileups have been linked to snow squalls, including a series of accidents on 22 February 2001 in Virginia, which included a 131-vehicle accident on Interstate 95 during whiteout conditions (DeVoir 2004). DeVoir referred to such events as “High Impact Sub Advisory (HISA)”, prior to the rollout of snow squall warning within the NWS. The National Weather Service (NWS) began issuing snow squall warnings (SQW) during the 2017–2018 cool season (NWS 2018). Prior to 2017–2018, the NWS did not have a practical method of highlighting snow squall events given legacy snow accumulation thresholds for winter weather advisory and winter storm warning criteria. NWS Weather Forecast Offices issue SQW based on the following criteria: (1) visibility

≤ 0.25 mi or less in snow with subfreezing ambient road temperatures, and (2) plunging temperatures sufficient to produce flash freezes and reductions of visibility from falling and/or blowing snow (NWS 2022). Furthermore, NWS meteorologist judgment regarding snow squall impacts, including time of day, day of week, and other societal factors, are considered within the SQW decision-making process (NWS 2022). The NWS does not have a set SQW wind speed and gust criteria, but rather relies on the judgment of meteorologists to assess the potential for significant reductions to visibility in the presence of gusty winds. As of 31 May 2022, the NWS has issued SQWs across the Intermountain West, the Four Corner States, the High Plains and Great Lakes regions, and across the Northeastern United States (IEM 2023; Fig. 1).

Previous snow squall literature has focused primarily across New England (Lundstedt 1993; DeVoir and Ondrejik 2008), the United States Midwest (DeVoir and Ondrejik 2008; Pettegrew et al. 2009), Wyoming and Colorado (Schumacher et al. 2010; Capella 2021), and Canada (Milrad et al. 2011, 2014). Snow squall climatology studies have been conducted across

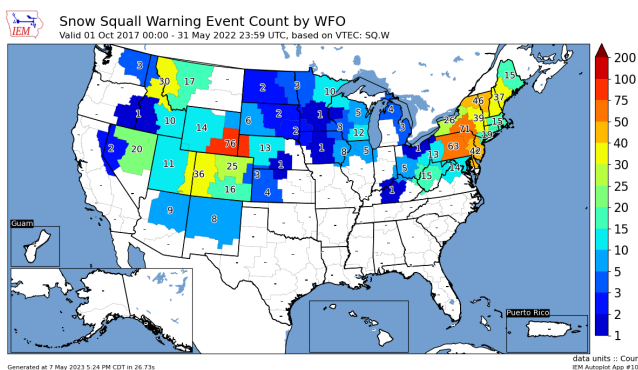


Figure 1. Snow squall warning event count by WFO, valid 0000 UTC 1 October 2017 – 0000 UTC 31 May 2022, across the CONUS. Graphic generated through via IEM data plotter (IEM 2023). *Click image for an external version; this applies to all figures hereafter.*

Vermont and northern New York (Banacos et al. 2014, herein known as B14), southern New England (Colby et al. 2022), and Wyoming (Capella 2021). B14 identified synoptic and mesoscale snow squall environments using a 10-yr climatology of snow squalls producing surface visibility ≤ 0.8 km (0.5 mi) from three sites over northern New York and Vermont. The synoptic environment was characterized by the cyclonic shear side of a mid-to-upper tropospheric jet streak within deep-layer cyclonically curved flow. B14 found a mesoscale environment defined by median surface-based convective available potential energy (SBCAPE) < 50 J kg $^{-1}$, within a high relative humidity 0–2-km AGL layer, frontogenetic forcing, and strong surface isallobaric (rise/fall) couplets. Colby et al. (2022) identified 100 snow squall events across southern New England from 1994 through 2018 and classified events into four categories: classic (squall movement from the northwest; 72 events), Atlantic (from the southwest; 15 events), Northern (from the north; 9 events), and Special (varying; 4 events). All snow squall cases were associated with cyclonic differential vorticity advection and often were associated with two-dimensional frontogenesis. Capella (2021) also investigated synoptic and mesoscale environments across 56 snow squall events at the Cheyenne Regional Airport (KCYS) in Wyoming, September – May, 2016–2021. Similar to B14, Capella (2021) found a synoptic environment characterized by a 500-hPa trough axis over KCYS and cyclonically curved flow within the left exit region of a ≥ 70 kt 300-hPa jet streak. Finally, Capella (2021) observed snow squalls driven by shallow upright convection, symmetric instability, and/or 700-hPa frontogenesis.

Snow squall research across the western CONUS also includes orographic snow band work, mainly in Montana. Orographic snow bands often deposit snow in long and narrow corridors, as documented by Hoenisch (2008), downstream of the Rocky Mountain Front in north-central Montana. On 12 January 2015, an orographic snow band brought snowfall rates in excess of 8 cm hr $^{-1}$ and led to the closure of Interstate I-90 east of Missoula (Johnson and Petrescu 2005). Orographic snow band impacts share similar characteristics to snow squalls, as travelers encounter abrupt visibility reductions in heavy snow and gusty winds. Using observations and model output, Kirshbaum and Durran (2005a, b) determined that flow-parallel orographic rainbands develop under weak moist instability and the cloud layer was associated with a unidirectional wind profile. Unidirectional mean flow (850–700-hPa) of 30–50-kt within a post-frontal cold air advection environment are essential to the generation of orographic snow bands (Petrescu 2003; Johnson and Petrescu 2005). Furthermore, the presence of a capping inversion and descending dry layer immediately above the moist and unstable 850–700-hPa cloud layer is necessary for convection to organize into orographic snow bands. In two snow band case studies—documented during December 2007—in north-central Montana, the synoptic environment was characterized by a relatively deep and unstable layer, a capping inversion in the mid-levels, 750–550-hPa unidirectional mean flow, and terrain anchor points to fix the location of orographic snow bands (Hoenisch 2008). Radar observations highlighted Rocky Mountain Peak as a terrain anchor point, as orographic snow bands initiated near the peak and remained nearly stationary through time, extending downstream into valley areas (Hoenisch 2008). Terrain anchor points were identified on radar imagery by finding areas with higher frequencies of quasi-stationary echoes in upslope areas (Hoenisch 2008).

Prior to Capella (2021), previous research across the western United States has lacked systematic searches for snow squall events. Past literature has focused on mesoscale banded precipitation and snowfall, prior to the rollout of snow squall warnings by the NWS in 2017–2018. This presents a challenge when reviewing prior research through the lens of snow squalls. Further education and outreach efforts are imperative for operational meteorologists and the public to understand the frequency and impacts of snow squalls.

Previous literature has not yet developed a climatology of snow squalls across western Montana.

Therefore, this research examined snow squalls across western Montana to: (1) develop a 20-yr climatology of snow squall events across western Montana, and (2) provide a framework for identifying synoptic environmental conditions associated with squalls to enhance NWS efforts to provide impact-based decision support services. Section 2 contains an overview of data including synoptic environment fields derived from the NCEP North American Regional Analysis (NARR; Mesinger et al. 2006). Section 3 highlights snow squall frequency and characteristics, and provides a discussion of the synoptic environment. Finally, section 4 provides a summary, an outline for future work, and recommendations for operational best practices for future events.

2. Data and methods

METAR data were retrieved from the Synoptic labs mesonet API (Synoptic Labs 2022) between October and April 2000–2020, at Missoula (KMSO), Kalispell (KGPI), and Butte, Montana (KBTM), to identify snow squall cases (Fig. 2). Surface data were filtered to identify peak wind gusts ≥ 26 kt (30 mph) and visibility ≤ 0.8 km (0.5 mi). The visibility threshold of ≤ 0.5 mi, which exceeds the NWS SQW criteria of ≤ 0.25 mi, was selected because ASOS visibility data has a higher bias at night compared to day for snowfall intensities (Rasmussen et al. 1999). Various wind speed criteria have been used previously by snow squall climatology studies including: (1) wind speed ≥ 0 kt (Capella 2021), (2) any increase in wind speed within a 1-hr period leading up to and including the squall (B14), and (3) wind speed ≥ 7 kt (Colby et al. 2022). Furthermore, NWS SQW criteria provides leeway to operational meteorologists when assessing wind speeds during snow squall events as no set wind speed criteria is specified (NWS 2022). For this study, peak wind gusts ≥ 26 kt were selected given the high likelihood for such speeds to create significant societal impacts from the combination of poor visibility in heavy snow and wind. Furthermore, using a lower-speed criteria, as done in previous studies, would have yielded a significantly higher number of events; whereas, the focus of this study is to identify squalls conducive to high societal impacts.

Snow squall cases were examined with NWS NEXRAD KMSX Doppler radar data retrieved from the Iowa State University Environmental Mesonet Archive



Figure 2. Regional map showing locations of ASOS sites used in this study along with United States Highways and Interstates [Kalispell, MT (KGPI); Missoula, MT (KMSO); and Butte, MT (KBTM)].

(IEM 2022) to determine if snowfall was associated with one or more convective bands, either with orographic snow bands or a defined frontal boundary (Fig. 3). Snow squall event types were classified by cross-referencing radar imagery, METAR observations, and synoptic environmental plots. Orographic snow bands were identified on radar imagery by finding long (≥ 80 km) and linear structures visually with continuous areas of at least 20 dBZ.

Snow squall characteristics, including event onset, duration of moderate and heavy snow (visibility ≤ 0.50 mi and ≤ 0.25 mi, respectively), 2-m temperature change, and peak wind gust were inspected. The 2-m temperature change was calculated by subtracting the minimum temperature during the snow squall, bounded by visibility ≤ 0.5 mi, and the maximum 2-m temperature within two hours of snow squall onset. In 68 of the 74 snow squall events, the duration of 2-m temperature change occurred within 3 hrs or less. Box and whisker plots were constructed for each site to identify similarities and differences among snow squall cases.

Snow squall events were also placed into three categories: orographic snow bands, Pacific cold fronts, and Canadian arctic cold fronts. Surface observations, KMSX radar imagery, and synoptic patterns were examined to classify each snow squall case. METAR wind direction criteria were applied to filter Pacific cold fronts (270–360-deg) and Canadian arctic fronts (270–360, 0–90-deg). Canadian arctic fronts at KBTM have a tendency to come across the Continental Divide from the north-northwest and east, depending on the depth of cold air. A composite study was conducted for each event type utilizing the NARR (NOAA Physical



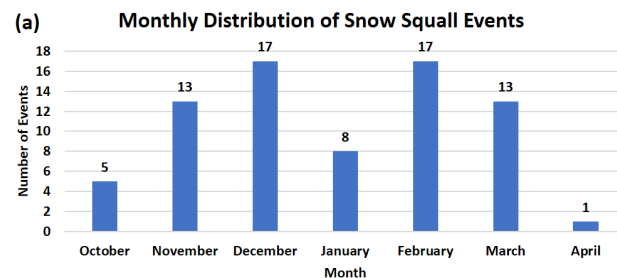
Figure 3. Missoula Nexrad Doppler Radar (KMSX) base reflectivity (dBZ) for a representative (a) Pacific cold front, (b) Canadian arctic front, and (c) orographic snow band snow squall cases. Yellow ovals highlight snow squalls within each case. Imagery retrieved via Iowa State IEM NEXRAD archive (IEM 2022).

Science Laboratory 2022). NARR mean composite maps times were constructed by finding the nearest time, in 3-hr increments (0000 UTC, 0300 UTC, etc.) prior to the onset of snow squalls. A review of historical NWS winter storm warning and winter weather advisory highlights was conducted in relation to each snow squall case.

3. Analysis

A total of 74 snow squall events were identified for KMSO, KGPI, and KBTM ASOS sites (Table 1). Table 1 also demonstrates that 30 of the snow squall events were not associated with NWS winter storm warning or winter weather advisory highlights. Of the 30 events without ongoing winter weather highlights, only 9 occurred after 2010. Following 2010, winter weather advisories were in effect for: 17 of 23 snow squall cases in KBTM, 5 of 7 in KMSO, and 8 of 9 at KGPI. Based on these trends, the rate of issuance for winter weather advisories prior to snow squall events has increased since 2010. In snow squall cases without winter weather highlights, 11 of the 30 occurred between 0100 UTC and 1200 UTC, typically during the overnight hours. Seven of the ten snow squall cases observed during a winter storm warning occurred at KGPI. Finally, 34 snow squall events occurred while a winter weather advisory was in effect. Furthermore, most cases ($n=42$) occurred between December and February (Fig. 4a). Snow squall events were most common between 1500 and 0100 UTC ($n=43$) and less common during the overnight hours (0200 UTC – 1400 UTC; 32 cases; Fig. 4b).

Three distinct snow squall event types were identified: orographic snow bands, Pacific fronts, and Canadian arctic fronts (Table 2). Every snow squall event at KGPI was associated with a Canadian arctic frontal passage and a north-northeast wind shift.



(b) Hourly Start Time Distribution of Snow Squall Events

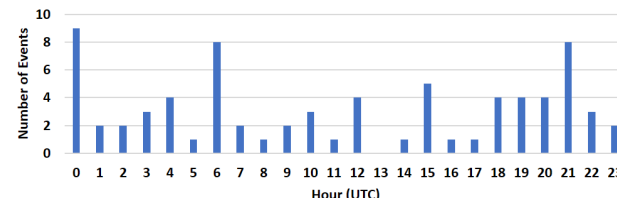


Figure 4. (a) Monthly and (b) hourly distributions of 74 snow squall events collected at Missoula, Kalispell, and Butte, MT from 2000–2020.

Orographic snow band events were limited to KMSO and KBTM. Careful analysis of KMSX radar imagery revealed zero orographic snow band events at KGPI through the climatology period. At KMSO, 9 of the 14 snow squall events were classified as orographic snow bands with prevailing winds out of the west to northwest. Pacific fronts ($n=25$) and orographic snow bands ($n=16$) dominate the snow squall events identified at KBTM. Winter weather highlights were not in effect for 17 of the 25 Pacific cold front events at KBTM.

The duration of moderate (visibility ≤ 0.50 mi) and heavy snowfall (visibility ≤ 0.25 mi), peak wind gusts, and 2-m temperature change ($^{\circ}\text{C}$) were examined. Consistent with work by B14, snow squalls across western Montana exhibit brief, but heavy snowfall. The interquartile range for duration of snow squalls with moderate snowfall was 24–45-min; in contrast, the interquartile range decreased to 15–35-min for heavy snowfall (Fig. 5). The majority of snow squall events were associated with heavy snowfall (i.e., 62 of 72 events). The median peak wind gust during each squall for KGPI, KMSO, and KBTM was 34-, 32-, 33-kt, respectively (Fig. 6). Four snow squall events at KBTM recorded peak wind gusts ≥ 43 kt (50 mph) and were associated with Pacific cold frontal passages.

A notable 2-m temperature change contrast existed within observing sites (Fig. 7). The interquartile range for 2-m temperature change at KGPI and KBTM was -2 to -7°C and -3 to -6°C , respectively, compared to

Table 1. Numerical breakdown of snow squall event types and NWS Winter Storm Warnings, Winter Weather Advisory, and no highlight frequency during observed snow squall cases at Missoula, Kalispell, and Butte, MT.

Location	Winter Storm Warning	Winter Weather Advisory	No Highlight
Missoula, MT (KMSO)	1	7	6
Kalispell, MT (KGPI)	7	9	1
Butte, MT (KBTM)	2	18	23

Table 2. Numerical breakdown of snow squall event types, including Pacific cold fronts, Canadian Arctic fronts, and snow band snow squalls for Missoula, Kalispell, and Butte, MT.

Location	Orographic Snow Bands	Pacific Cold Fronts	Canadian Arctic Fronts
Missoula, MT (KMSO)	9	3	2
Kalispell, MT (KGPI)	0	0	17
Butte, MT (KBTM)	16	25	2

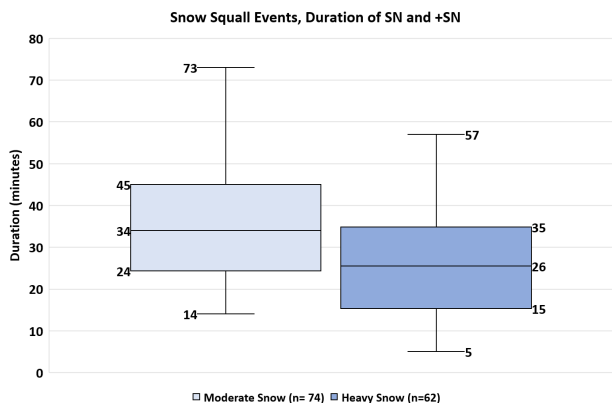


Figure 5. Box-and-whiskers plot portraying the duration of moderate ($VSBY \leq 0.50$ SM) and heavy snow ($VSBY \leq 0.25$ SM) for 74 snow squall events across western Montana reported by ASOS sites KMSO, KBTM, and KGPI. Filled boxes represents the interquartile range (25th to 75th percentile), and the end of the whiskers show the 10th and 90th percentile values. Sample size denoted by n .

-1.5 to -3.5°C for KMSO. In 11 of the 17 snow squalls events observed at KGPI, the antecedent temperature was $\geq 0^{\circ}\text{C}$. Across KGPI snow squall cases, the median 2-m temperature before and during the snow squalls was -1.1°C and -6.1°C , respectively, and was associated with an interquartile range of -3.3°C to 2.8°C and -7.3°C to -2.7°C , respectively. In contrast, the median antecedent surface temperature of 1.7°C at KBTM is warmer than KGPI, with 31 of the 43 events identified, observing a temperature $\geq 0^{\circ}\text{C}$. During a 3-h period, 25 of the 43 snow squall KBTM events observed a $\geq 4^{\circ}\text{C}$

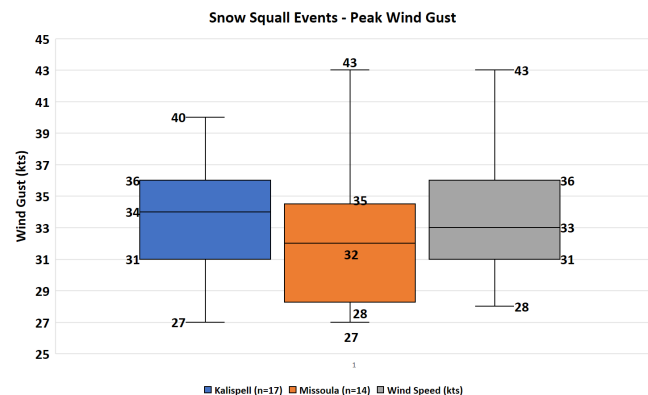


Figure 6. As in Fig. 4, except for observed peak wind gusts (kts) during snow squall events.

temperature drop. The 2-m temperature environment at KGPI and KBTM highlights the threat for flash freezes during snow squalls, as antecedent 2-m temperatures near or above freezing quickly drop below freezing as the snow squall occurs.

a. Orographic snow bands synoptic analysis

An examination of NARR composite mean 500-hPa maps during orographic snow band events ($n=25$) highlight an upper-level trough axis moving across western Montana prior to squall onset (Fig. 8a). Upstream of the trough axis, an upper-level ridge was building offshore the Pacific Northwest. The aforementioned short-wave trough is moving eastward across central Montana (Fig. 8a). NARR 300-hPa fields reveals a northwesterly cyclonic flow pattern across western Montana during orographic snow band snow

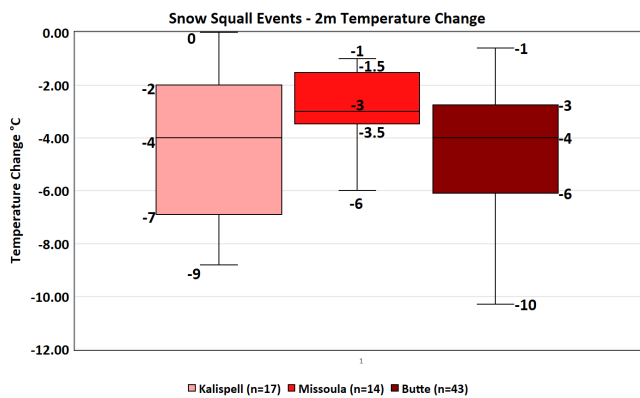


Figure 7. As in Fig. 4, except for observed 2-m temperature change ($^{\circ}\text{C}$) during snow squall events. The 2-m temperature change was calculated by subtracting the minimum temperature during the snow squall bounded by visibility ≤ 0.50 mi and the maximum 2-m temperature within two hours of snow squall onset.

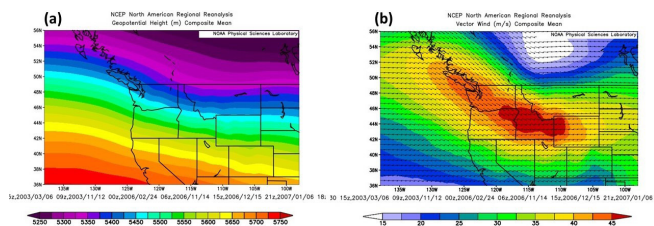


Figure 8. NARR composite (a) 500-hPa mean geopotential heights (m, color filled) and (b) 300-hPa vector wind speed (m s^{-1} , color filled) for orographic snow band snow squall events ($n=25$) observed across western Montana.

squall events (Fig. 8b). In the NARR mean composites, west-central and southwestern Montana were located in the left exit region of a $40\text{--}45\text{ m s}^{-1}$ jet streak centered in southern Idaho.

NARR 850-hPa and 700-hPa mean wind fields feature a unidirectional westerly flow during orographic snow banding events (Fig. 9). 700-hPa and 850-hPa westerly winds of 35–40-kt and 20–25-kt were estimated, respectively. Therefore, the 850–700-hPa mean flow was on the order of 30 kt, near the low end of Petrescu (2003) recommended threshold of 30–50 kt for heavier band cases. In the 6-hrs following orographic snow band observations, the 700-hPa wind shifted to the northwest, leading to an increase in wind shear between 850 and 700-hPa. Following band development, rising 500-hPa heights were estimated across western Montana. A 50-dam height rise was estimated across western Montana 12-hrs following orographic snow band observations with an apparent positively tilted

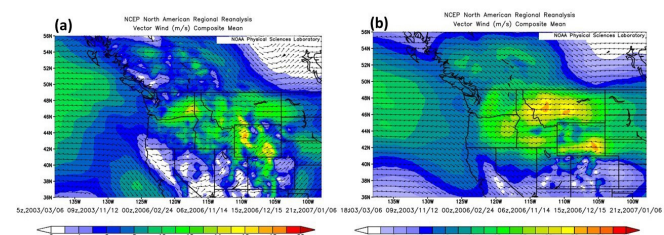


Figure 9. NARR composite (a) 850-hPa mean vector wind speed (m s^{-1} , color filled) and (b) 700-hPa vector wind speed (m s^{-1} , color filled) for orographic snow band snow squall events ($n=25$) observed across western Montana.

ridge axis in place across eastern Washington. NARR mean composite SCAPE fields reveal $60\text{--}80\text{-J kg}^{-1}$ across Clearwater and Idaho Counties in north-central Idaho (Fig. 10a), with a $30\text{--}40\text{-J kg}^{-1}$ axis of instability present across western Montana. Mean SCAPE values decreased to $20\text{--}30\text{-J kg}^{-1}$ 6-hrs after orographic snow band onset and diminished to 10 J kg^{-1} 12 hrs after onset.

b. Pacific cold fronts synoptic analysis

NARR mean composite 500-hPa fields for Pacific cold front events ($n=28$) revealed a short-wave trough axis centered near the Idaho and Washington border (Fig. 11a). A review of 300-hPa NARR composite fields placed western Montana in the left exit region of a $40\text{--}45\text{-ms}^{-1}$ zonal westerly jet centered across southern Oregon and Idaho (Fig. 11b). Downstream, an upper-level ridge axis was present across eastern Montana and the High Plains. Analysis of the 700-hPa and 850-hPa temperature (Fig. 12a) fields revealed a frontal zone with vertical continuity moving across western Montana. Modest cold air advection is ongoing, given 700-hPa temperature falls of $5\text{--}6\text{ }^{\circ}\text{C}$ in the 6-hr period leading to squall onset. NARR mean composite charts suggest a surface low was present across the Idaho Panhandle prior to the onset of Pacific cold front snow squalls with a 300-hPa trough axis extending southeastward across western Montana (Fig. 12b). A close examination of NARR mean composite MSLP fields suggests a 10-hPa pressure rise was estimated across western Montana during a 6-hr period during and following the snow squall along the Pacific cold frontal boundary. Across western Montana, mean SCAPE values of $60\text{--}80\text{-J kg}^{-1}$ were estimated (Fig. 10b). Finally, it's worth noting that these mean composite values were higher than the median SCAPE values found in snow squalls across

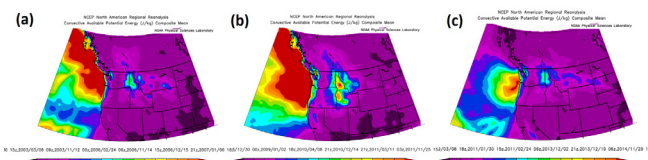


Figure 10. NARR composite mean SBCAPE (J kg^{-1}) for (a) orographic snow band, (b) Pacific cold front, and (c) Canadian arctic front snow squall cases.

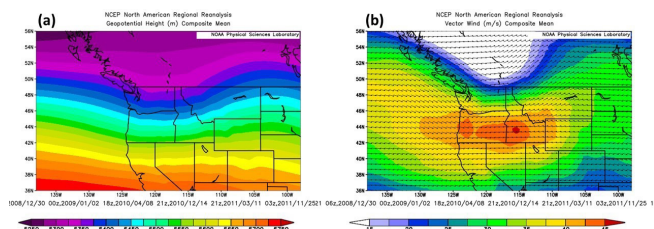


Figure 11. NARR composite (a) 500-hPa mean geopotential heights (m, color filled) and (b) 300-hPa vector wind speed (m s^{-1} , color filled) for pacific cold front snow squall events ($n=28$) observed across western Montana.

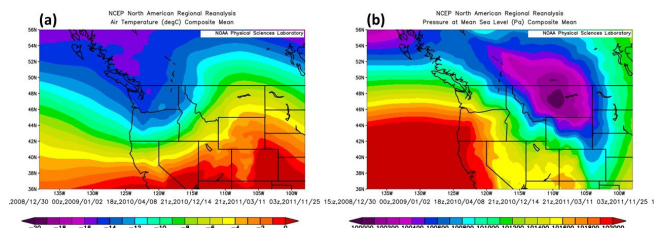


Figure 12. NARR composite (a) 700-hPa mean Air Temperature ($^{\circ}\text{C}$, color filled) and (b) mean MSLP (Pa, color filled) for pacific cold front snow squall events ($n=28$) observed across western Montana.

northern New York and Vermont (36 J kg^{-1} ; B14).

c. Canadian arctic fronts synoptic analysis

NARR composite mean 500-hPa geopotential height fields for Canadian arctic front events ($n=21$) revealed a different synoptic pattern compared to Pacific cold front events. A high amplitude blocking pattern was evident across the Pacific off the western United States and British Columbia coast (Fig. 13a). The ridge axis extends poleward along the Alaska and Canadian border. A zonal flow pattern was apparent across the eastern United States. NARR mean composite 500-hPa fields across the western United States, British Columbia and Alberta revealed a positively tilted trough axis extending across eastern Washington northeastward near Calgary, Canada. At 300-hPa, a $40\text{--}45\text{-m s}^{-1}$ anticyclonic jet

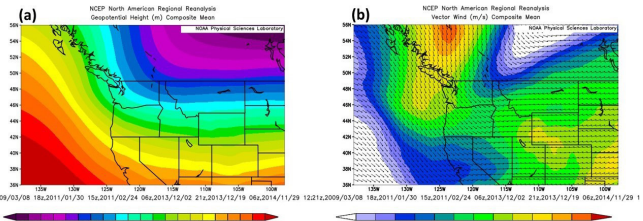


Figure 13. NARR composite (a) 500-hPa mean geopotential heights (m, color filled) and (b) 300-hPa mean vector wind speed (m s^{-1} , color filled) for Canadian cold front snow squall events ($n=21$) observed across western Montana.

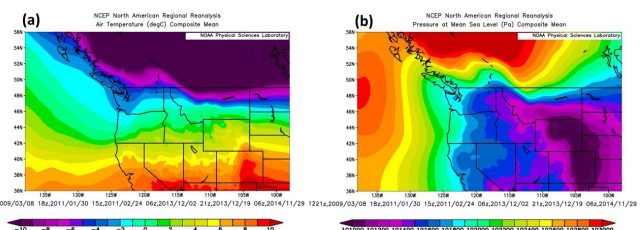


Figure 14. NARR composite (a) 850-hPa mean air temperature ($^{\circ}\text{C}$, color filled) and (b) mean MSLP (Pa, color filled) for Canadian arctic front snow squall events ($n=21$) observed across western Montana.

was estimated across British Columbia (Fig. 13b). The trough axis present at 500-hPa, extends upwards to 300-hPa, with weak $15\text{--}20\text{-m s}^{-1}$ northwesterly flow present across northwestern Montana.

NARR mean composite 850-hPa air temperature and MSLP fields revealed an arctic cold front propagating across the Continental Divide into western Montana (Fig. 14). 850-hPa model fields across northwest Montana depicted a westerly to northerly wind shift was ongoing. Anecdotally, deeper arctic cold front passages across northwestern Montana were often associated with 700-hPa northeast winds on the order of $20\text{--}30\text{-m s}^{-1}$, while NARR composite 700-hPa winds were on the order of 6 m s^{-1} . NARR MSLP fields revealed a U-shaped ridge across north-central Montana as the arctic front propagated eastward along the Continental Divide (Fig. 14b). A 10-hPa gradient is present along the Continental Divide as a surface trough is apparent across west-central Montana. NARR mean composite SBCAPE values associated with Canadian arctic front snow squall events across western Montana were between $30\text{--}40\text{-J kg}^{-1}$ and align with values in B14 (Fig. 10c).

4. Conclusions

A 20-yr climatology of snow squalls and associated synoptic patterns was examined across three ASOS sites in western Montana: Missoula (KMSO), Kalispell (KGPI), and Butte (KBTM). This study built on existing snow squall climatology studies by B14, Colby et al. (2022), and Capella (2021) in the Northeastern United States and Wyoming. The criteria used to identify snow squalls within this climatology (wind gusts ≥ 26 kt and visibility ≤ 0.5 mi) match higher end events, where SQW criteria was clearly met. A total of 74 snow squall cases were identified, with 42 events occurring between 1500 and 0100 UTC. The median duration of heavy (moderate) snow during snow squalls was 26 (34) min. The median peak wind gust during snow squalls at KGPI, KMSO, and KBTM was 34-, 32-, 33-kt, respectively. Snow squalls across western Montana fall into three categories based on their synoptic environment: orographic snow bands, Pacific cold fronts, and Canadian arctic fronts. Orographic snow band events were characterized by unidirectional westerly flow, weak moist instability environments ($\text{SBCAPE} \leq 80 \text{ J kg}^{-1}$), and rising heights following the onset of snow squall events. These banding events share similar synoptic characteristics as previous work by Petrescu (2003), Johnson and Petrescu (2005), and Hoenisch (2008). Pacific cold front events were associated with the passage of an upper-level trough, a frontal zone with vertical continuity, and occur on the cyclonic shear side of an upper-tropospheric jet streak. Surface temperatures in the majority of Pacific cold front events cross the freezing mark during the onset of heavy snow and gusty winds, creating an environment favorable for flash freeze risk on untreated area roadways. Of the 21 Canadian arctic front snow squall cases, 17 occurred at KGPI, with only two cases at KMSO and KBTM. Canadian arctic front cases were highlighted by a sudden north-northeast wind shift, temperature drop, and poor visibility in heavy snow and wind. As with Pacific cold fronts, the surface temperature environment was favorable for flash freezes. This study provides operational meteorologists in western Montana a framework for assessing snow squall synoptic pattern types. Future research is needed to develop a climatology of snow squalls meeting NWS SQW criteria across the rest of Intermountain West.

Acknowledgments. The author thanks Chris Gibson for his helpful review and suggestions and to Bruce Bauck for his support of the project. The NARR composite images were created via the NOAA/ESRL Physical Sciences Division from their website (<https://psl.noaa.gov/cgi-in/data/narr/plothour.pl>). WSR-88D base reflectivity images were generated through the Iowa State University Iowa Environmental Mesonet online archive (<https://mesonet.agron.iastate.edu/>). The views expressed in this paper are those of the authors and do not necessarily reflect those of NOAA or the NWS.

REFERENCES

Banacos, P. C., A. N. Loconto, and G. A. DeVoir, 2014: Snow squalls: Forecasting and hazard mitigation. *J. Operational Meteor.*, **2** (12), 130–151, [CrossRef](#).

Capella, R. J., 2021: An improved environmental forecast parameter for snow squalls in the High Plains and Mountain West, University of Wyoming Department of Atmospheric Science, 2021.

Colby, F. P., Jr., D. Coe, M. Barlow, R. Brown, and E. Krajewski, 2022: A climatology of snow squalls in southern New England 1994–2018, *Monthly Weather Review*, **150** (7), 1541–1561, [CrossRef](#).

DeVoir, G. A., 2004: High impact sub-advisory snow events: the need to effectively communicate the threat of short duration high intensity snowfall. *20th Conf. on Weather Analysis and Forecasting/16th Conf. on Numerical Weather Prediction*, Seattle, WA, Amer. Meteor. Soc., 10.2, [CrossRef](#).

DeVoir, G. A., and D. Ondrejik, 2008: NWS expands efforts to mitigate effects of high impact sub-advisory (HISA) snowfall in central Pennsylvania. NWS State College, PA, Spring 2008 Media Newsletter, 4 pp, [CrossRef](#).

Hoenisch, R., 2008: Convective snow banding over north central Montana. *Western Region Technical Attachment Lite*, No. 8-8, [CrossRef](#).

IEM, 2022: Iowa Environmental Mesonet NEXRAD base reflectivity archive. Department of Agronomy, Iowa State University, Accessed 12 September 22. [Available online at <https://mesonet.agron.iastate.edu/nws/>]

—, 2023: Iowa Environmental Mesonet automated data plotter. Department of Agronomy, Iowa State University, Accessed 13 May 2023. [Available online at <https://mesonet.agron.iastate.edu/plotting/auto/?q=109>]

Johnson, M. W., and E. Petrescu, 2005: January 2005 banded snow event using the weather event simulator. *Western Region Technical Attachment Lite*, No.5-14, [CrossRef](#).

Kirshbaum, D. J. and D. R. Durran, 2005a: Observations and modeling of banded orographic convection. *J. Atmos. Sci.*, **62**, 1463–1479, [CrossRef](#).

—, 2005b: Atmospheric factors governing banded orographic convection. *J. Atmos. Sci.*, **62**, 3758–3774, [CrossRef](#).

Lundstedt, W., 1993: A method to forecast wintertime instability and non-lake effect snow squalls across northern New England. *Eastern Region Technical Attachment*, No. 93-11A, [CrossRef](#).

Mesinger, F., and Coauthors, 2006: North American regional reanalysis. *Bull. Amer. Meteor. Soc.*, **87**, 343–360, [CrossRef](#).

Milrad, S. M., J. R. Gyakum, E. H. Atallah, and J. F. Smith, 2011: A diagnostic examination of the eastern Ontario and western Quebec wintertime convection event of 28 January 2010. *Wea. Forecasting*, **26**, 301–318, [CrossRef](#).

—, —, K. Lombardo, and E. H. Atallah, 2014: On the dynamics, thermodynamics, and forecast model evaluation of two snow-burst events in southern Alberta. *Wea. Forecasting*, **29**, 725–749, [CrossRef](#).

NOAA Physical Science Laboratory, 2022: 3-Hourly NCEP North American regional reanalysis (NARR) composites. Accessed 12 September 2022. [Available online at <https://www.esrl.noaa.gov/psd/cgi-bin/data/narr/plothour.pl>]

NWS, 2018: Snow squall warnings now available nationwide: alerts aimed at reducing vehicle crashes and road fatalities. Accessed 22 September 2022. [Available online at <https://www.noaa.gov/stories/snow-squall-warnings-now-available-nationwide>]

—, 2022: WFO winter weather products specification 10-513: Accessed 13 May 2023. [Available online at <https://www.nws.noaa.gov/directives/sym/pd01005013curr.pdf>]

Petrescu, E., 2003: Analysis of the November 11th, 2003 convective snow banding event in Western Montana using the weather event simulator, *Western Region Technical Attachment Lite*, No. 03-55, [CrossRef](#).

Pettegrew, B. P., P. S. Market, R. A. Wolf, R. L. Holle, and N. W. S. Demetriades, 2009: A case study of severe winter convection in the Midwest. *Wea. Forecasting*, **24**, 121–139, [CrossRef](#).

Rasmussen, R. M., J. Vivekanandan, J. Cole, B. Myers, and C. Masters, 1999: The estimation of snowfall rate using visibility. *J. Appl. Meteor.*, **38**, 1542–1563, [CrossRef](#).

Schumacher, R. S., D. M. Schultz, and J. A. Knox, 2010: Convective snowbands downstream of the Rocky Mountains in an environment with conditional, dry symmetric, and inertial instabilities. *Mon. Wea. Rev.*, **138**, 4416–4438, [CrossRef](#).

Synoptic Labs, 2022: Mesonet API Web Services Documentation. Accessed 12 September 2022. [Available online at <https://developers.synopticdata.com/mesonet/v2/>]